Acta Crystallographica Section A
Foundations of Crystallography
ISSN 0108-7673

Received 26 June 2013
Accepted 13 August 2013

Homometry in the light of coherent beams

Sylvain Ravy

Synchrotron-Soleil, L'Orme des Merisiers, Saint-Aubin BP48, 91192 Gif-sur-Yvette, France.
Correspondence e-mail: ravy@synchrotron-soleil.fr

Two systems are homometric if they are indistinguishable by diffraction. A distinction is first made between Bragg and diffuse scattering homometry, and it is shown that in the last case coherent diffraction can allow the diffraction diagrams to be differentiated. The study of the Rudin–Shapiro sequence, homometric to random sequences, allows one to manipulate independently two-point and four-point correlation functions, and to show their effect on the statistics of speckle patterns. This study provides evidence that long-range order in high-order correlation functions has a measurable effect on the speckle statistics.

1. Introduction

The possibility to shape coherent X-ray beams from synchrotron light sources (Livet, 2007) and to get naturally coherent beams of soft (Vartanyants *et al.*, 2011) and hard X-rays (Gutt *et al.*, 2012) from X-ray free-electron lasers (XFELs) has revolutionized the way X-ray diffraction experiments are performed and analysed. One of the most fascinating properties of coherent diffraction is the possibility of measuring speckle patterns (Sutton *et al.*, 1991; Livet, 2007), which are much more informative than the diffuse scattering obtained by classical diffraction. Together with the development of novel sources, phase retrieval algorithms have also emerged, allowing reconstruction of the diffracting objects under certain experimental conditions (Miao *et al.*, 1999; Rodenburg & Faulkner, 2004). However, reconstruction of a structure is not always possible nor necessary to study the physics of materials. For example, measuring correlation lengths close to phase transitions (Ravy *et al.*, 2007) or slow dynamics with X-ray photon correlation spectroscopy (Livet, 2007; Grübel & Zontone, 2004) does not require the full reconstruction of the system under study.

The purpose of this paper is to show that statistical analysis of speckle patterns can yield information on orders hidden to conventional X-ray analysis, because they are induced by high-order correlation functions. In this respect, we are in line with recent works showing that four-point intensity cross-correlation of speckle patterns can uncover 'hidden symmetries' present in colloidal glasses (Wochner *et al.*, 2009) or magnetic systems (Su *et al.*, 2011).

Our approach uses the concept of homometry, *i.e.* the property of different systems to exhibit the same diffraction patterns. In §2, we first separate out the scattered intensity expression into three terms, which allows us to show that homometry, introduced in §3, can occur at different levels. In §4, we show that coherent diffraction can help in solving some Bragg homometry situations. We then put the emphasis on diffuse scattering homometry (§5), which we discuss with the help of the Rudin–Shapiro sequence (Axel *et al.*, 1992; Baake & Grimm, 2009). The results are discussed in §7.

2. Coherent diffraction

Let us first give a general expression of the intensity scattered at scattering vector q, by a one-dimensional periodic N-site lattice decorated by two atoms A and B, of scattering factors f_A and f_B, in proportions x and $1-x$, respectively. Generalization to two dimensions, three dimensions, multi-atomic basis, displacement disorder, or disorder of the second kind (Guinier, 1994) is straightforward. Following Guinier (1994), the diffracted intensity is given by

$$I(q) = \sum_{n,n'} f_n f_{n'} \exp[iq(n'-n)] = \sum_m \sum_n f_n f_{n+m} \exp(iqm). \quad (1)$$

The *ensemble* average of the product $\langle f_0 f_m \rangle$ is then introduced:

$$\frac{1}{N_m} \sum_n f_n f_{n+m} = \langle f_0 f_m \rangle + \Delta_m, \quad (2)$$

where N_m is the m-dependent number of terms of the sum $\sum_n$. The Δ_m term, usually neglected in textbooks, is due to finite size fluctuations of the spatial average with respect to the *ensemble* one.

Further introduction of $\Delta f_m = f_m - \langle f \rangle$ allows one to get the three components of kinematic diffraction:

$$I_{\rm B}(q) = \langle f \rangle^2 \sum_m N_m \exp(iqm) \quad (3)$$

$$I_{\rm DD}(q) = \sum_m N_m \langle \Delta f_0 \Delta f_m \rangle \exp(iqm) \quad (4)$$

$$I_{\rm S}(q) = \sum_m N_m \Delta_m \exp(iqm). \quad (5)$$

The first term gives the intensity of the Bragg reflections and the fringes due to finite size effects. For a crystal of N cells of structure factor $F(q)$, it can be written as:

$$I_{\rm B}(q) = |\langle F(q)\rangle|^2 \frac{\sin^2 q(N+1)/2}{\sin^2 q/2}. \quad (6)$$

In practice, the fringes given by the sine functions are only visible with a coherent beam illumination [for conditions of observation and examples, see Livet (2007)].

The second term is the diffuse scattering intensity, which only depends on the pair correlation function (CF). For *random* disorder, it reduces to the well known Laue formula:

$$I(q) = Nx(1-x)(f_A - f_B)^2, \quad (7)$$

where *random* refers to the vanishing of the pair CF (*i.e.* $\langle \Delta f_0 \Delta f_m\rangle = \langle \Delta f_0\rangle\langle \Delta f_m\rangle = 0$ for $m \neq 0$).

The third term gives rise to speckles. Like fringes, speckles only exist if the incident beam is coherent enough, *and* if the system does not explore too many configurations during acquisition time T (non-ergodicity condition $\langle \Delta_m\rangle_T \neq 0$). Interestingly enough, working out of coherent conditions has the effect of averaging out Δ_m, which yields *ensemble* averaged quantities.

3. Homometry

Homometry – etymologically *same distance* – is a word coined by Patterson (1939, 1944) to describe the property of sets of points, neither congruent nor enantiomorphic, which possess the same pair distances (or the same difference sets) (Senechal, 2008). Homometric sets thus have the same diffraction pattern, as demonstrated by equation (1). A simple example of homometry is given by the two sets $S = \{0, 1, 4, 10, 12, 17\}$ and $S' = \{0, 1, 8, 11, 13, 17\}$ (Senechal, 2008). Indeed, their structure factors $F(q)$ have the same magnitude for *all* q vectors, but not the same phase. Hence, the loss of the phase makes these sets *indistinguishable* by X-ray diffraction.

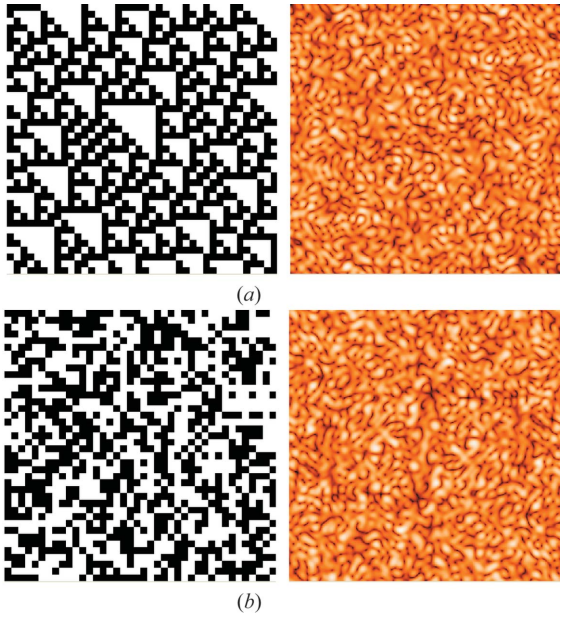

Figure 1
(Left) (40 × 40) lattices of +1 and −1 in equal proportion and (right) corresponding speckle patterns in the first Brillouin zone (log scale) for (*a*) a triplet SRO lattice (Welberry & Butler, 1994), (*b*) a random lattice. Reciprocal nodes are in the corners.

However, because solid-state physics deals with materials, the above definition turns out to be too restrictive. Equation (2) allows one to distinguish between Bragg, B-homometry, the property of different systems to have the same Bragg reflection intensities, and diffuse scattering, D-homometry, the property of having the same diffuse scattering. We will reserve the term homometry (or true homometry) for situations where coherent diffraction speckle patterns are similar. For the sake of consistency, let us first discuss the B-homometry.

4. Bragg homometry: a solvable case

B-homometry describes crystals with a different basis but the same Bragg intensities (Patterson, 1939, 1944). A finer distinction was made by Hosemann & Bagchi (1954), who introduced pseudo-homometric structures, *i.e.* crystals which are homometric only in the infinite limit. To illustrate that, let us consider the examples of one-dimensional homometric crystals presented in Patterson (1944), of unit-cell size equal to 8 and atomic positions given by $H = \{0, 3, 4, 5\}$ and $H' = \{0, 4, 5, 7\}$. Structure factors, readily calculated as

$$F_H(q) = 1 + 2\cos q + \exp(i4q) \quad (8)$$

$$F_{H'}(q) = 2(\cos q + \cos 2q), \quad (9)$$

have the same amplitude squared *at* the Bragg positions $q = h(2\pi/8)$ (h integer) but not *out of* Bragg positions. Equation (6) shows that the fringe intensity, revealed by coherent diffraction, gives out-of-Bragg values of $|F(q)|^2$ which, at least in theory, allow one to distinguish H and H', and solves the B-homometry issue.

This is well known and corresponds to the oversampling requirement of the phase retrieval algorithms (Sayre, 1952; Miao *et al.*, 1998; van der Veen & Pfeiffer, 2004). It is clear however that if the atomic basis is homometric itself, like *e.g.* in crystals with an S or S' basis, the problem cannot be solved, coherence or not.

5. Diffuse scattering homometry: new aspects

Because it is related to high-order CFs and local order in disordered systems, D-homometry is of fundamental interest. A surprising illustration of D-homometry was discussed by Welberry (1977) and Welberry & Butler (1994). In these papers, the authors designed substitutionally disordered lattices with triplet (or quadruplet) short-range-ordered (SRO) CFs,[1] but zero two-point correlations (Fig. 1*a*). Diffraction diagrams of these lattices display the same Bragg and diffuse scattering intensities (Welberry & Butler, 1994), as expected from equations (3) and (4), clearly illustrating the well known fact that diffuse scattering is not sensitive to high-order CFs g_k, $k > 2$.

[1] In the following, we consider that an order parameter is short-range ordered (SRO) if its associated correlation function $g(n)$ vanishes at infinity and long-range ordered (LRO) otherwise.

In order to check the homometry properties of such disordered lattices, we calculated the coherent diffraction patterns by fast Fourier transforms (FFTs) of the (zero-padded) random and triplet-SRO lattices shown in Fig. 1. The coherent diffraction patterns of both lattices clearly exhibit speckles with constant average intensity but different speckles repartition, which shows that coherent diffraction breaks the D-homometry, at least qualitatively.

In this part, we will address the issue of finding *quantitative criteria* to show the presence of high-order CFs in speckle patterns. However, high-order CFs are much less intuitive than pair CFs and also much more difficult to manipulate. Indeed, systems with well characterized high-order CFs have not been explored as much as two-point SRO or LRO ones and there are very few appropriate examples in the literature. In the following, we will show that the geometrically ordered (GO) (Gratias *et al.*, 2005) Rudin–Shapiro (RS) sequence (Gratias & Axel, 1995) is well adapted to this task because it is D-homometric to random sequences, and exhibits long-range order in its four-point (or quadruplet) CFs.

The generic term σ_n can be written (Baake & Grimm, 2009)

$$\sigma_{4n+l} = \begin{cases} \sigma_n & \text{for} \quad l = 0, 1 \\ (-1)^{n+l}\sigma_n & \text{for} \quad l = 2, 3 \end{cases} \quad \text{with } \sigma_0 = 1. \qquad (10)$$

This sequence has become famous (Axel *et al.*, 1992; Höffe & Baake, 2000; Gratias & Axel, 1995; Gratias *et al.*, 2005) because, though GO, it has the same diffuse scattering as that of randomly distributed sequences [sometimes called Bernoulli sequences (BSs) (Höffe & Baake, 2000)], given by the $4Nx(1-x)$ Laue formula [equation (7)]. In other words, its two-point CF $g_2(n) = \overline{\sigma_0\sigma_n}$ is zero for $n \neq 0$ (*spatial* average).

Let us now consider the coherent diffraction of RS and Bernoulli sequences. In what follows, we present FFT computations of sequences of length N, zero-padded up to a value $M \gg N$ to clearly see the speckles. For the RS sequence, because $x \neq 0.5$ and depends on its length N, we have always subtracted the average value $2x - 1$ from all the terms in order to get rid of the Bragg intensites. BSs of 1 and -1 in equal proportion were computed with the python pseudo-random number generator. The squared value of the FFT $I(q)$ are normalized by $4Nx(1-x)$ in order to get $\overline{I(q)} = 1$.

Fig. 2 shows the diffraction patterns of RS and Bernoulli sequences in the first Brillouin zone ($0 < q < 2\pi$). Inspection of these patterns shows that, although their average value is the same, the speckle repartition is remarkably different. In particular, it is clear that the BS pattern exhibits many more spikes, while the RS pattern is more homogeneous and regular: there are no low- or high-intensity speckles and they are more regularly spaced. To quantify this observation, we studied the statistics of both speckle patterns by calculating their probability density of intensity $P(I)$. It is known that for a random media (see *e.g.* Dainty, 1976), the intensity distribution has a negative exponential distribution given by

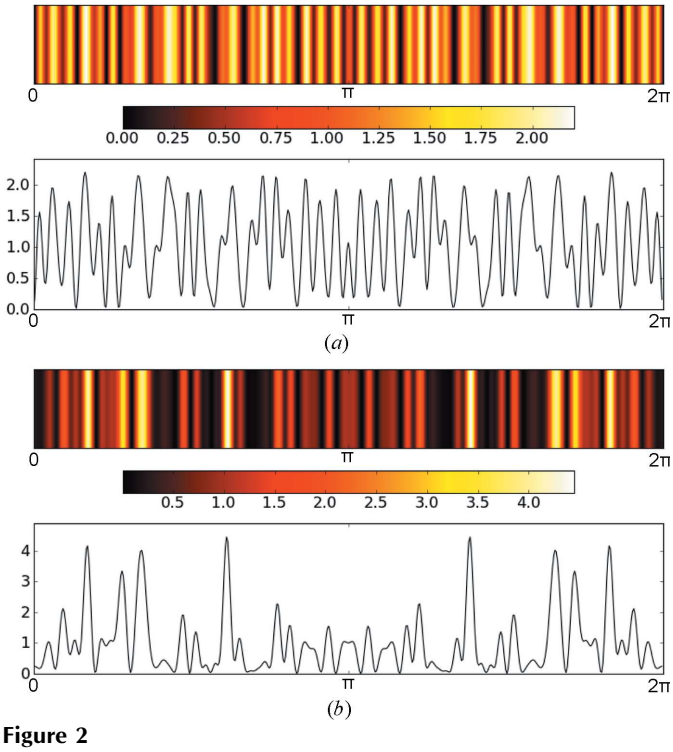

Figure 2
Speckle patterns and associated intensity variations from $[(N, M) = (64, 512)]$ (*a*) RS and (*b*) Bernoulli sequences. The vertical broadening of the patterns are for visual convenience.

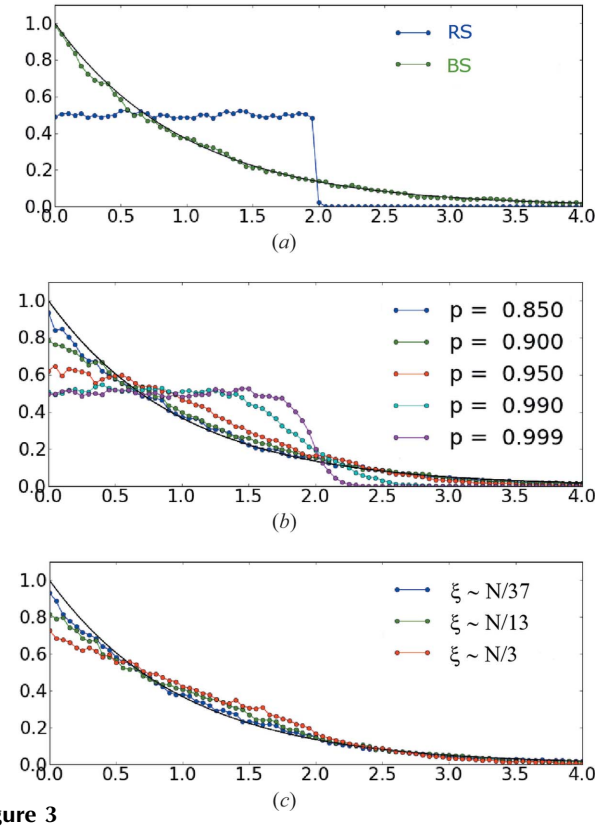

Figure 3
Probability densities $P(I)$ of speckle patterns of $(N, M) = (4096, 4096 \times 128)$: (*a*) BS (green) and RS sequence (blue), (*b*) sequences obtained by Bernoullization for different p, (*c*) g_4 SRO sequences for different ξ. The line indicates the random negative exponential law.

$$P(I) = \frac{1}{\bar{I}} \exp -\frac{I}{\bar{I}}, \tag{11}$$

which in our case reduces to $P(I) = \exp(-I)$.

Fig. 3(*a*) shows the probability densities $P(I)_{\rm RS}$ and $P(I)_{\rm BS}$ for the RS and Bernoulli sequences. While $P(I)_{\rm BS}$ follows quite well the negative exponential law, as expected, this is not the case for $P(I)_{\rm RS}$. Though the precision of $P(I)_{\rm RS}$ depends on N, it is well approximated by the step function $P(I<2) = 0.5$. This statistic, which means that intensities lower than 2 occur with the same probability, explains the homogeneous aspect of the diffraction pattern. The quantitative difference between both statistics clearly shows that the presence of GO, invisible through diffuse scattering, is revealed by the statistics of the speckle pattern, breaking the D-homometry in a quantifiable way.

In order to better understand this behaviour, we have quantified the degree of order of the RS by one of its quadruplet CFs, namely the pair–pair CF:

$$g_4(n) = \overline{\sigma_0\sigma_1\sigma_n\sigma_{n+1}}. \tag{12}$$

Indeed, we first checked that the RS triplet CF $g_3(n,n') = \overline{\sigma_0\sigma_n\sigma_{n'}}$ is zero and does not show any structure. We found that the quadruplet CFs are the first relevant high-order CFs to characterize the RS order. Amongst them, we chose $g_4(n)$ because it is reminiscent of the very definition of σ_n given by equation (10). Moreover, pair–pair CFs give information on bond orientational order, which is of physical interest in two-dimensional systems such as hexatic liquid crystals (Bruinsma & Nelson, 1981), and has recently been investigated with respect to coherent diffraction (Altarelli *et al.*, 2010).

We found numerically that, at variance with the BS, $g_4(n)$ is LRO for the RS sequence (Fig. 4*a*). This is confirmed by the behaviour of its FFT $\hat{g}_4(q)$ (Fig. 4*b*), which exhibits well defined peaks indexed by the basis vectors $\{(h_i/4.2^i)|h_i \in \{-1,1\}, i \in N\}$, characteristic of limit-periodic functions (Baake & Grimm, 2011). This behaviour has been checked up to the $N = 2^{14}$ RS sequences. By analogy with two-point orders, we define $\eta_4 \equiv \hat{g}_4(\pi/2)^{1/2}/N = 1/2$ as the order parameter of this sequence.

Let us now study the $P_{\rm RS}(I)$ behaviour as a function of disorder. We first decreased η_4 while keeping g_4 LRO *and* g_2 disorder by using the 'Bernoullization' procedure as defined in Baake & Grimm (2009). It consists in changing the sign of each σ_n with probability $1-p$, in order to build sequences intermediate between the pure RS ($p = 0, 1$) and Bernoulli ($p = 0.5$) sequences. The order parameter η_4 was found numerically to vary as $\eta_4(p) \simeq (1-2p)^2/2$. Note that this procedure only decreases the order parameter while keeping the g_4 LRO, the same way an anti-ferromagnetic (AF) order parameter (for example) would decrease without breaking the AF LRO. In this last case however, the order parameter decreases as $\sim (1-2p)$, which shows that quadruplet order is more sensitive to disorder than two-point order.

Typical probability density curves shown in Fig. 3(*b*) exhibit a continuous evolution as a function of p. The step-function behaviour is rapidly lost as $p \to 0.5$, with the best sensitivity close to the small intensity values $P(I=0)$. Fig. 5 shows the behaviour of $P(I=0)$ as a function of p, computed from an $N = 1024$ sequence, together with the $1-2\eta_4(p)^2$ curve. Most importantly, it appears that $P(I=0)$ directly follows the quadruplet order parameter squared and is consequently a clear signature of the quadruplet order. This *demonstrates* that high-order CFs can be shown by X-ray coherent diffraction.

However, because the Bernoullization procedure keeps the quadruplet LRO, this remarkable result should be tested against SRO. The effect of g_4 SRO on the speckle pattern was studied by shifting the sequence by two lattice periods at certain points, randomly selected with probability $1-p$. This ensures we achieve g_4 SRO, clearly seen by the broadening of the $\hat{g}_4(\pi/2)$ peak, *while keeping* the $g_2(n)$ correlation to zero. Fig. 3(*c*) shows the results for different average distances between faults ξ. It appears that $P(I)_{\rm BS}$ is almost unaffected by the quadruplet SRO for $\xi < N/40$. This shows that the extent of the quadruplet order has a much larger effect on the speckle statistics than the Bernoullization procedure. In other words, while decreasing the RS order gives a sizeable and measurable effect on the density probability of the speckle pattern, breaking LRO rapidly destroys the speckle statistics

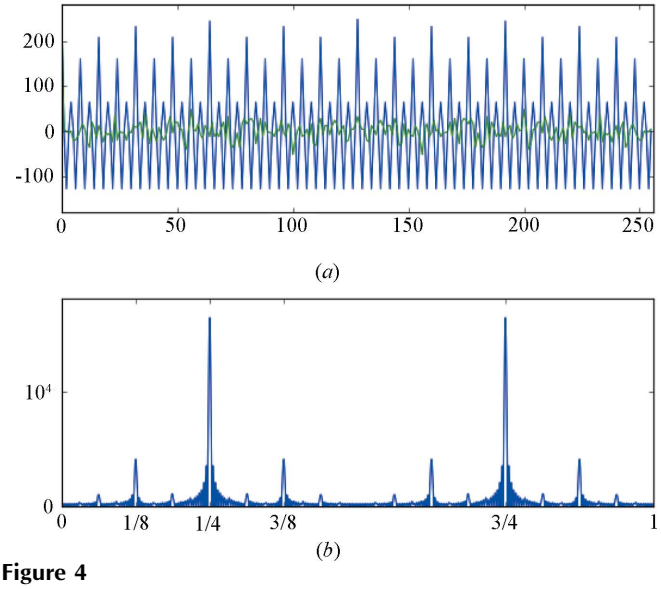

Figure 4
(*a*) Computed $g_4(n)$ using periodic boundary conditions for $N = 256$ RS sequence (blue) and a Bernoulli sequence (green). (*b*) Magnitude of RS $\hat{g}_4(q)$ as a function of $h = q/2\pi$.

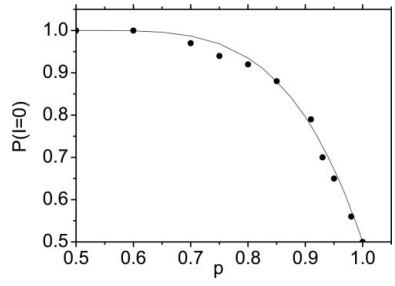

Figure 5
$P(I=0)$ as a function of the probability p, calculated for an $N = 1024$ lattice. The line corresponds to the $1-2\eta_4(p)^2$ curve, as explained in the text.

of the ordered state, making evidence of high-order CFs more difficult to obtain.

6. True homometry

Because it is related to the difficult issue of unicity in inverse problems, true homometry is beyond the scope of this paper. For the sake of completeness however, let us mention the discussion given in Rodenburg (1989) and the fact that using ptychography (Rodenburg & Faulkner, 2004), in which diffraction patterns are obtained by shifting illumination on the sample, can solve difficult problems of phase retrieval (Guizar-Sicairos *et al.*, 2010), including true homometry.

7. Discussion

It might seem pointless to discuss the problem of homometry while phase retrieval algorithms and ptychography can provide the full structural information, and thus high-order correlation functions. However, the full measurement of three-dimensional speckle patterns is time consuming and in many situations it is not possible to get the data. For example in 'one-shot' XFEL experiments, the speckle pattern obtained will be a two-dimensional cut of the reciprocal space, which prevents full three-dimensional reconstruction. Similarly, it will be quite difficult to get three-dimensional patterns of rapidly evolving systems such as liquids, liquid crystals or colloids. Methods of speckle analyses on such quickly measured patterns are thus needed to get novel information on the materials.

As stressed in Schneider *et al.* (2010), real cases of true B-homometry are rare. In contrast, because disorder is involved, D-homometry is very common especially when systems are large. Moreover it is related to high-order CFs which are hardly accessible to experiments (Wochner *et al.*, 2009; Su *et al.*, 2011; Treacy *et al.*, 2005).[2] The purpose of this numerical study was to demonstrate that high-order CFs have a measurable effect on the speckle statistics obtained by coherent diffraction. To this end, we have first shown that the RS sequence, which is D-homometric to random sequences, is long-range ordered in its quadruplet CFs, and we have defined an associated order parameter. By disordering the sequence while keeping the pair CF constant, the high-order CFs have been shown to give rise to measurable effects on speckle pattern statistics, as shown by the behaviour of the probability density of intensity $P(I)$ (Figs. 3*a*, 3*b*). This conclusion is reinforced by the curve displayed in Fig. 5 where $P(I = 0)$ is shown to follow the quadruplet order parameter squared. Finally, breaking down LRO by adding phase defects also breaks the statistics for a few percentage of defects, as shown in Fig. 3(*c*). Qualitatively, the 'spikiness' of speckle patterns is quickly reinforced by the introduction of defects, which makes deviation to the negative exponential curve difficult to observe. The conclusion of this study is that LRO high-order CFs have indeed a quantifiable effect on $P(I)$, but that SRO high-order CFs are more difficult to show.

Using this technique to analyse speckle patterns can be difficult for experimental reasons. First, the presence of two-point correlations in all real systems (the classical SRO) could obviously mask the speckle distribution analysis. In this respect, we have checked that, at least for SRO lattices with no high-order correlations, dividing the speckle pattern intensity by its associated diffuse scattering one $I_{\rm DD}$ (by smoothing, averaging or fitting) makes $P(I/I_{\rm DD})$ follow the normal decreasing exponential law. This can help in disentangling high-order effects from two-point ones.

Another issue might be the partial coherence of the beam, which reduces the speckle contrast and makes the previous analyses difficult. This could be overcome by the analysis of the speckle maximum intensities, which exhibit similar statistical properties.

Coming back to the two-dimensional disordered lattices presented in §5, we checked that the probability density of the speckle patterns shown in Fig. 1(*b*) does not present sizeable deviation from the negative exponential distribution. This is consistent with the previous conclusions that high-order CFs must present enough LRO to have a measurable effect on $P(I)$ (the average size of the white triangles, characteristic of the triplet order, is only a few lattice constants). However, the simple fact that the lattices of Fig. 1 can be reconstructed with minimum information with phase retrieval algorithms shows that high-order CFs are hidden in the speckle repartition. This remark obviously calls for a theoretical effort to find the relevant parameters (SRO correlation lengths, CF order *etc.*) controlling the speckle statistics in any system. Such an effort could be supported by more sophisticated numerical analyses such as the use of second-order (or higher) probability functions (Dainty, 1976). In this respect, algorithmic approaches using basic constraints could be an alternative approach.

We hope this work will provide an impetus for theoretical and experimental studies on the relation between high-order CFs and speckle statistics.

We thank F. Berenguer, D. Gratias, D. Le Bolloc'h and F. Livet for useful discussions.

[2] Let us emphasize that the techniques developed in Treacy *et al.* (2005) to get high-order CFs require sample scanning, as in ptychography.

References

Altarelli, M., Kurta, R. P. & Vartanyants, I. A. (2010). *Phys. Rev. B*, **82**, 104207.
Axel, F., Allouche, J. & Wen, Z.-Y. (1992). *J. Phys. Condens. Matter*, **4**, 8713–8728.
Baake, M. & Grimm, U. (2009). *Phys. Rev. B*, **79**, 020203.
Baake, M. & Grimm, U. (2011). *Philos. Mag.* **61**, 2661–2670.
Bruinsma, R. & Nelson, D. R. (1981). *Phys. Rev. B*, **23**, 402–410.
Dainty, J. C. (1976). *The statistics of speckle patterns*. In *Progress in Optics*, Vol. XIV. Amsterdam: North Holland.
Gratias, D. & Axel, F. (1995). Editors. *Beyond Quasicrystals.* Berlin: Springer Verlag.
Gratias, D., Bresson, L. & Quiquandon, M. (2005). *Annu. Rev. Mater. Res.* **35**, 75–98.
Grübel, G. & Zontone, F. (2004). *J. Alloys Compd.* **362**, 3–11.

Guinier, A. (1994). *X-ray Diffraction in Crystals, Imperfect Crystals and Amorphous Bodies*. New York: Dover Publications.
Guizar-Sicairos, M., Evans-Lutterodt, K., Isakovic, A. F., Stein, A., Warren, J. B., Sandy, A. R., Narayanan, S. & Fienup, J. R. (2010). *Opt. Express*, **18**, 18374–18382.
Gutt, C. *et al.* (2012). *Phys. Rev. Lett.* **108**, 024801.
Höffe, M. & Baake, M. (2000). *Z. Krystallogr.* **215**, 441–444.
Hosemann, R. & Bagchi, S. N. (1954). *Acta Cryst.* **7**, 237–241.
Livet, F. (2007). *Acta Cryst.* A**63**, 87–107.
Miao, J., Charalambous, P., Kirz, J. & Sayre, D. (1999). *Nature (London)*, **400**, 342–344.
Miao, J., Sayre, D. & Chapman, H. N. (1998). *J. Opt. Soc. Am. A*, **15**, 1662–1669.
Patterson, A. L. (1939). *Nature (London)*, **143**, 939–940.
Patterson, A. L. (1944). *Phys. Rev.* **65**, 195–201.
Ravy, S., Le Bolloc'h, D., Currat, R., Fluerasu, A., Mocuta, C. & Dkhil, B. (2007). *Phys. Rev. Lett.* **98**, 105501.
Rodenburg, J. M. (1989). *Ultramicroscopy*, **27**, 413–422.
Rodenburg, J. M. & Faulkner, H. M. (2004). *Appl. Phys. Lett.* **85**, 4795.
Sayre, D. (1952). *Acta Cryst.* **5**, 843.
Schneider, M. N., Seibald, M., Lagally, P. & Oeckler, O. (2010). *J. Appl. Cryst.* **43**, 1012–1020.
Senechal, M. (2008). *Eur. J. Combin.* **29**, 1933–1944.
Su, R., Seu, K. A., Parks, D., Kan, J. J., Fullerton, E. E., Roy, S. & Kevan, S. D. (2011). *Phys. Rev. Lett.* **107**, 257204.
Sutton, M., Mochrie, S. G. J., Greytak, T., Nagler, S. E., Berman, L. E., Held, G. A. & Stephenson, G. B. (1991). *Nature (London)*, **352**, 608–610.
Treacy, M. M. J., Gibson, J. M., Fan, L., Paterson, D. J. & McNulty, I. (2005). *Rep. Prog. Phys.* **68**, 2899–2944.
Vartanyants, I. A. *et al.* (2011). *Phys. Rev. Lett.* **107**, 144801.
Veen, F. van der & Pfeiffer, F. (2004). *J. Phys. Condens. Matter*, **16**, 5003.
Welberry, T. R. (1977). *J. Appl. Cryst.* **10**, 344–348.
Welberry, T. R. & Butler, B. D. (1994). *J. Appl. Cryst.* **27**, 205–231.
Wochner, P., Gutt, C., Autenrieth, T., Demmer, T., Bugaev, V., Ortiz, A. D., Duri, A., Zontone, F., Grübel, G. & Dosch, H. (2009). *Proc. Natl Acad. Sci. USA*, **106**, 11511–11514.